MEDIUM-ENERGY PROTON-NUCLEUS ELASTIC SCATTERING IN THE IMPULSE APPROXIMATION

P. Schwandt, F. Petrovich* and A. Picklesimer

Following KMT[1], the central (C) and spin-orbit (LS) parts of the first-order optical potential for proton-nucleus scattering in the impulse approximation (IA) are calculated as the convolution of nuclear formfactors $\rho_i(q) = \int \rho_i(r)\exp(-i\vec{q}\cdot\vec{r})\, d\vec{r}$ with two-nucleon transition matrices $t_{pi}(q)$ where $i = p,n$ and q is the momentum transfer; $\rho_i(r)$ is the nuclear density distribution normalized to $\int \rho_p(r)d\vec{r} = Z$, $\int \rho_n(r)d\vec{r} = N$.

For a spin-zero nucleus (spin-saturated shells) this prescription defines the potential in configuration space explicitly as

$$U(r) = U_c(r) + \frac{1}{r}\frac{d}{dr} U_{LS}(r)\, \vec{L}\cdot\vec{\sigma} \qquad (1)$$

$$= \frac{A-1}{A}\frac{\eta}{2\pi^2}\int q^2 [\rho_p(q)<t^c_{pp}(q)> + \rho_n(q)<t^c_{pn}(q)>]$$

$$j_0(qr)\, dq + i\frac{A-1}{A}\frac{\eta}{2\pi^2}\frac{k_{cm}}{k_{CM}}\int q^4[\rho_p(q)<t^{LS}_{pp}(q)>$$

$$+ \rho_n(q)<t^{LS}_{pn}(q)>]\frac{j_1(qr)}{qr}\, dq\, \vec{L}\cdot\vec{\sigma}$$

where $\eta \equiv \varepsilon^2/E_1\cdot E_2$ arises from relating the 2-body t-matrix in the nucleon-nucleon (NN) barycentric system (cm) to the corresponding quantity in the nucleon-nucleus barycentric system (CM); here ε is the total energy of each interacting nucleon in cm and E_1, E_2 the nucleon total energies in CM, and k_{cm}, k_{CM} are the corresponding momenta.

The $<t^C_{pi}>$, $<t^{LS}_{pi}>$ represent the central and two-particle spin-orbit transition matrices averaged in spin and isospin over the A target nucleons, i.e., in terms of the 2-nucleon channel spin S, isospin T elements t_{TS}:

$$<t^c_{pp}> = \frac{1}{4}(t^c_{10} + 3t^c_{11}), \quad <t^c_{pn}> = \frac{1}{8}(t^c_{00} + 3t^c_{01} + t^c_{10} + 3t^c_{11}) \qquad (2)$$

$$<t^{LS}_{pp}> = t^{LS}_{11}, \quad <t^{LS}_{pn}> = \frac{1}{2}(t^{LS}_{01} + t^{LS}_{11})$$

One-nucleon exchange is an important component of the proton-nucleus interaction at low and medium energies. In its general form the fully antisymmetrized 2-nucleon t-matrix is a sum of direct (D) and exchange (E) parts:

$$t_{TS}(q,p) = t^D_{TS}(q) + (-1)^{T+S+1} t^E_{TS}(p) \qquad (3)$$

where $q = |\vec{k} - \vec{k}'|$ and $p = |\vec{k} + \vec{k}'|$. This off-shell t-matrix leads to a non-local potential. To obtain the local potential of eq. (1), we use a common approximation technique[2] to incorporate the effect of exchange which consists of evaluating $t^E(p)$ at $p = k_{CM}$ in the overlap integral (effectively ignoring the bound-nucleon momentum variable in the Fourier transform of t).

In configuration space the transition operator in each 2-body channel TS is generally expressed as an expansion in terms of Yukawa radial formfactors with various ranges R_i. In momentum space this yields the expansion

$$t^c_{TS}(q,k) = \sum_i V^c_{i,TS}[F_i(q,\mu_i) + (-1)^{T+S+1}F_i(k,\mu_i)]$$

$$t^{LS}_{T1}(q,k) = \sum_i V^{LS}_{i,TS}[G_i(q,\mu_i) + (-1)^{T+S+1}G_i(k,\mu_i)] \qquad (4)$$

where

$$F(q,\mu) \equiv \frac{4\pi/\mu}{q^2+\mu^2}, \quad G(q,\mu) \equiv \frac{8\pi/\mu}{[q^2+\mu^2]^2}, \quad \mu \equiv 1/R$$

and the V_i are complex effective interaction strengths.

Two parametrizations of this t-matrix expansion were considered in the present analysis: one due to Love[3], the other due to Picklesimer and Walker[4] (P+W). The former had been constructed by adjusting the 12 complex strengths $V^{C(LS)}_{1,TS}$, $V^{C(LS)}_{2,TS}$ of the short-range components ($R_1 = 0.25$ fm, $R_2 = 0.40$ fm) to reproduce the 140 MeV NN phase shift solution of McGregor, Arndt and Wright[5], with the 4 central, long-range

parts $V_{3,TS}^C$ for $R_3 = 1.414$ fm taken as real and fixed at the appropriate OPEP values, for a total of 28 t-matrix parameters. In the P+W parametrization both ranges R_i and strengths V_i for each spin-, iso-spin-component were free parameters, adjusted to produce a satisfactory overall fit to the 50-400 MeV NN differential cross section and polarization data directly, for a total of 21 central and LS terms. One important distinction between these two constructions of the NN transition operator is that the P+W parametrization emphasized the large-q range in fitting nucleon-nucleon data, while in the calculation of the optical potential for a large nucleus the low-q behaviour of the t-matrix dominates the folding integral (1).

The dependence of the optical potential on the proton and neutron densities is clearly exhibited in (1). For the present initial study of the applicability of the IA to proton-elastic scattering at 100-200 MeV from ^{40}Ca, ^{90}Zr and ^{208}Pb we have used the best available phenomenological densities. Calculations with microscopic (e.g. Hartree-Fock) densities are in progress. The phenomenological density distributions used here are parametrized as

$$\rho_i(r) = \rho_{oi} \frac{1 + w_i r^2/R_i^2}{1 + \exp\,[(r^k - R_i^k)/a_i^k]} + C_i \exp\,[-r^2/b_i^2]$$

where $i = p,n$ and $R = r_o A^{1/3}$. The parameters for the nuclei studied here are displayed in Table 1. They were determined in recent IA analyses of proton elastic scattering data (cross section and polarization) at 0.8 GeV[6] (^{90}Zr, ^{208}Pb) and 1.0 GeV[7] (^{40}Ca) using a spin-dependent NN scattering amplitude. For proton scattering by medium and heavy nuclei at these energies the higher-order corrections to the first-order optical potential are expected to be sufficiently small to permit reliable extraction of nuclear matter distributions, subject only to uncertainties in the NN amplitude parametrization.

Table 1

	r_{op}	a_{op}	r_{on}	a_{on}	w_p	w_n	k	$C_{p,n}$	$b_{p,n}$
^{40}Ca	1.075	.585	1.053	.590	-.10	-.10	1	–	–
^{90}Zr	1.015	2.41	1.002	2.45	.32	.56	2	–	–
^{208}Pb	1.089	2.56	1.045	3.13	.36	.36	2	.13	2.18

With the nucleon densities and t-matrices parametrized as described, the convolution integrals (1) were evaluated. The resulting complex optical potentials were then used in a relativistically modified Schrödinger equation[8] to calculate angular distributions of elastic scattering observables for comparison with the recent IUCF data[9] on ^{40}Ca, ^{90}Zr, and ^{208}Pb at proton energies of about 121-135, 160, and 180 MeV.

Some typical results from the early stages of the ongoing study are presented here. Fig. 1 illustrates the characteristic q-dependence of the real t-matrix components Re $<t_{pi}^C>$, Re$<t_{pi}^{LS}>$ (here for the Love parametrization at 182 MeV; a weak dependence on proton energy arises through k in the exchange approximation) in relation to the nucleon formfactor for a heavy nucleus (here $\rho_p(q)$ for ^{208}Pb); clearly only the low-q range ($q \lesssim 2$ fm^{-1}) contributes significantly to the convolution integral, as was pointed out earlier.

Again for p + ^{208}Pb at 182 MeV, in fig. 2 comparison is made between the IA results for the optical potentials and the phenomenological potentials (OM) of ref. 9, with the obvious notation $U_c(r) = V(r) + iW(r)$, $U_{so}(r) = V_{so}(r) + iW_{so}(r)$. Both the Love and P+W formulations of the t-matrix are presented here. A number of interesting observations can be made:

(1) the IA results for the Love and P+W t-matrices are in good agreement with each other except for the real central term $V(r)$ which is considerably weaker and has a somewhat smaller rms radius in the P+W case. This may in part be due to our approximation made in the exchange term. A look at the contributions to ReJ_c
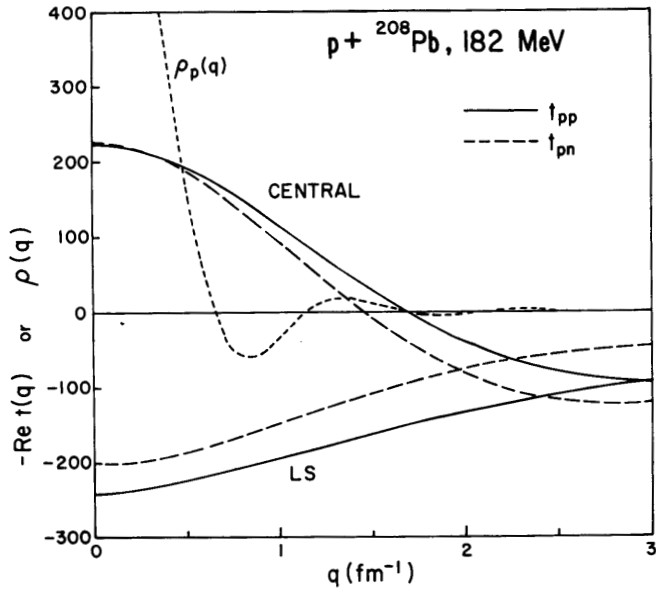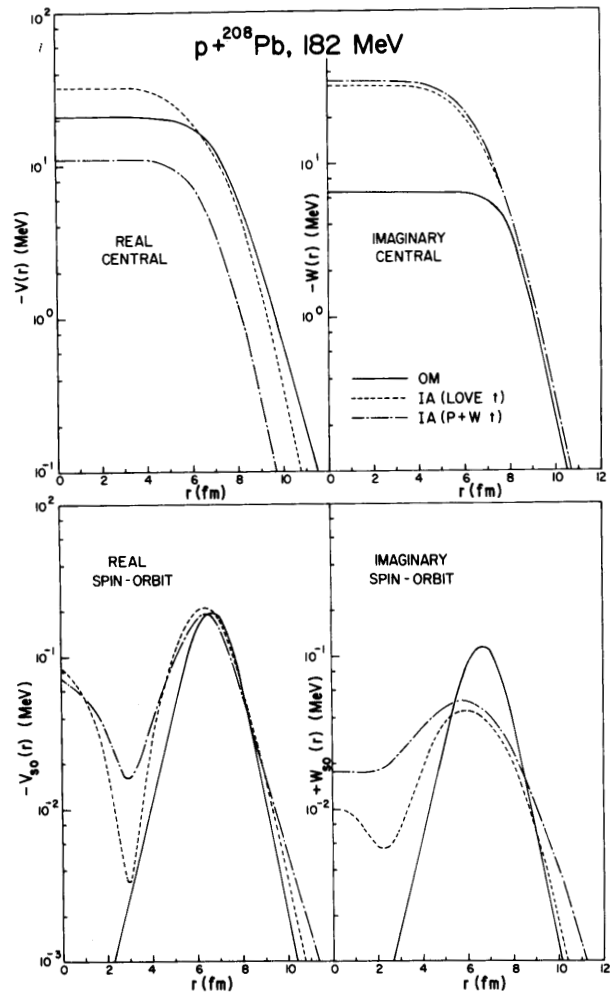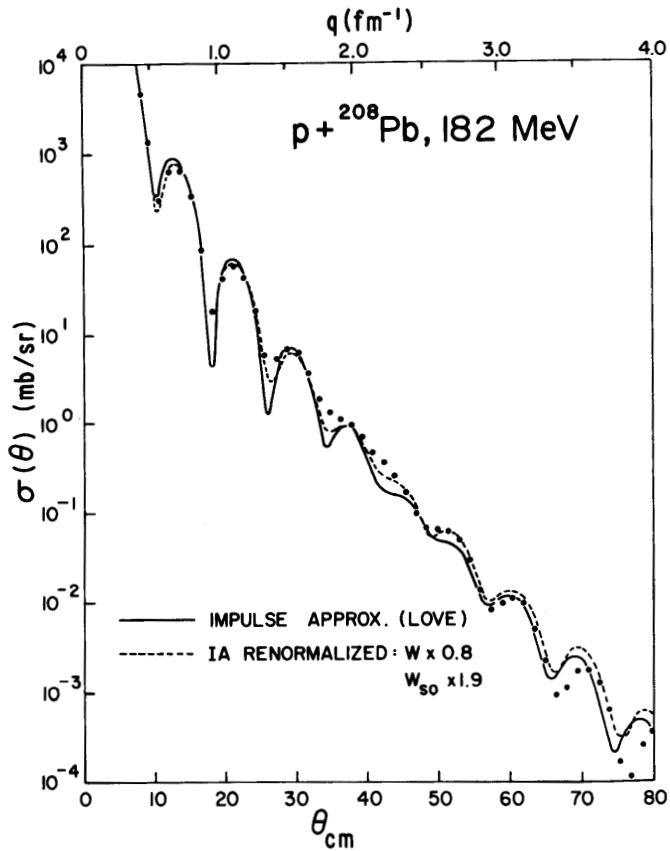
Figure 1.

Figure 2.

Figure 3.
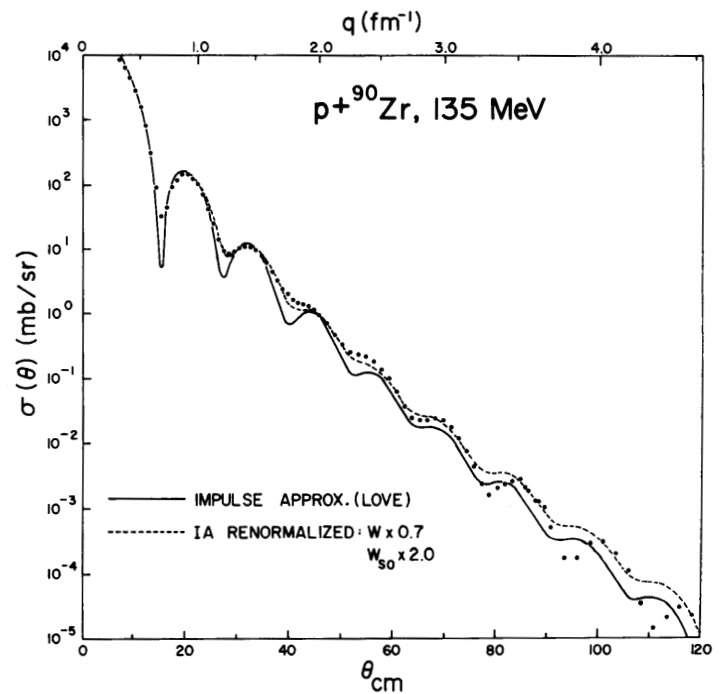

Figure 4.

(the volume integral per nucleon of V(r), eq.(6)) by the individual spin, isospin components of t in table 2 reveals that for the common choice p=k for the exchange momentum variable the attractive even-parity components (TS=10,01) for the P+W parametrization is smaller by roughly a factor 2 relative to the Love results, and the absence of the attractive triplet-odd (11) component in the P+W force further reduces its total attraction. We also find the attractive even-parity contributions to ReJ_c to be relatively more sensitive to the choice of p for the P+W parametrization of the t-matrix than for the Love formulation.

Table 2

| | ReJ_c (MeV – fm^3) | |
TS	Love	P+W
10	−102	−50
01	−152	−90
00	+88	+73
11	−40	0
Total	−206	−67

(2) The imaginary central strength W(r) obtained in the IA is far larger in the nuclear interior than the phenomenological OM result. A much smaller deviation in the same direction is also observed for the real central part V(r). For both V(r) and W(r) good agreement is found between IA and OM in the low-density surface region of the nucleus.

(3) For the real spin-orbit term V_{so} (r) excellent agreement in both radial shape and strength is found for IA and OM results (the differences in shape for r < 3 fm are largely unobservable and hence irrelevant since the significant surface partial waves are excluded from that radial region by the angular momentum barrier and absorption).

(4) The IA result for the imaginary spin-orbit term W_{so}(r) in the surface region is about a factor 2 smaller than the OM result.

The problem with V(r) for the P+W result, and the discrepancies between OM and IA for the imaginary central and spin-orbit strengths common to both t-matrix parametrizations, are reflected in varying degrees in the calculated differential cross sections. Surprisingly, the large difference in W(r) in the nuclear interior appears to have less serious consequences on the cross section than anticipated. In figs. 3 and 4 the IA results are compared to the experimental cross sections for ^{90}Zr at 135 MeV and ^{208}Pb at 182 MeV, respectively. The solid curve in each case represents the direct result for the Love t-matrix; the dashed curves illustrate the improvement in fit to the data achieved by a renormalization of the imaginary central and spin-orbit strengths W, W_{so} by the factors indicated. The unrenormalized IA potentials clearly provide a satisfactory description of the scattering for momentum transfers q ≡ 2ksin(θ/2) up to q ~ 3.5 fm^{-1}. At larger scattering angles the magnitudes and angular positions of the data oscillations are not well reproduced. A simple renormalization of the strengths does not cure this particular problem but provides a significant improvement in the fit for q $\lesssim$ 3 fm^{-1}, as expected, since the renormalization brings the IA potentials into closer agreement with the OM potentials for r $\gtrsim$ $R_{1/2}$ (the half-density radius).

Table 3 provides a representative comparison of the potential volume integrals

$$J_c \equiv \frac{1}{A}\int 4\pi r^2 U_c(r)dr, \qquad J_{so} \equiv \frac{1}{A^{1/3}}\int 4\pi r^2 U_{so}(r)dr \tag{6}$$

(in MeV-fm^3) and the corresponding rms radii (in fm) between IA and OM for the two cases illustrated, ^{90}Zr at 135 MeV and ^{208}Pb at 182 MeV (the IA results are for the Love t-matrix without renormalization).

Table 3

	p + ^{90}Zr, 135 MeV		p + ^{208}Pb, 182 MeV	
	IA	OM	IA	OM
Re J_c	-242	-224	-206	-186
Im J_c	-203	-117	-204	-73
Re J_{so}	-57	-97	-53	-45
Im J_{so}	12.5	43	14.4	27
$<r^2>^{1/2}_{c,R}$	4.65	5.03	5.89	6.37
$<r^2>^{1/2}_{c,I}$	4.58	5.22	5.81	6.63
$<r^2>^{1/2}_{so,R}$	5.28	5.15	6.90	7.04
$<r^2>^{1/2}_{so,I}$	5.40	5.15	6.96	7.04

For both cases, the rms radii for the central potentials are significantly smaller for the IA than for the OM which compensates partly for the difference in potential strengths in the central region.

Results of calculations using the P+W t-matrix are not represented here since the present calculations, involving an approximate and possibly oversimplified treatment of exchange, will be superceded by calculations with correct treatment of exchange. When compared with the data, the present P+W t-matrix calculations are distinctly worse than the results shown in figs. 3 and 4.

Continuation of this study of proton elastic scattering at medium energies in the IA will involve the following extensions and improvements of the present calculations:

(1) the use of an energy-dependent form of the Love t-matrix. The present parametrization is based on 140 MeV NN scattering; Love has recently constructed similar t-matrices fitted to 100 and 200 MeV NN phase shifts.[10]

(2) exact treatment of exchange for the P+W t-matrix. The necessary computer coding is currently being undertaken by one of the authors (AP) of that t-matrix.

(3) the use of a density-dependent 2-body interaction. The present IA formulation does not take account of the Pauli principle in the central, high-density region of the target nucleus.

(4) exploration of the sensitivity of the IA results to alternative (e.g., microscopic) nuclear density distributions.

(5) comparison of the IA predictions of polarization to experimental data as reliable polarization data become available at proton energies above 100 MeV.

1) A.K. Kerman, M. McManus and R.M. Thaler, Ann. Physics 8, 551 (1959).

2) F. Petrovich et al., Phys. Rev. Lett. 22, 895 (1969).

3) W.G. Love et al., Phys. Lett. 73B, 277 (1978).

4) A. Picklesimer and G.E. Walker, Phys. Rev. C17, 237 (1978).

5) M.H. McGregor, R.A. Arndt and R.M. Wright, Phys. Rev. 182, 1714 (1969).

6) L. Ray et al., Phys. Rev. C18, 1756 (1978); ibid, Phys. Rev. C18, 2641 (1978).

7) A. Chameaux, V. Layly and R. Schaeffer, Phys. Lett. 72B, 33 (1977).

8) P. Schwandt, "Elastic Scattering Analysis Code SNOOPY6", IUCF Int. Rep. No. 77-8 (1977).

9) P. Schwandt et al., IUCF Techn. and Scient. Report 1977, pp. 79-84; ibid., BAPS 23, 593 (1978).

10) W.G. Love, private communication.